

# Influence of Temperature with its Geometric and Failure Morphology Defects on the Mechanical Properties of Graphene: Molecular Dynamics Simulation (MDs)

Prabhu Paramasivam

Received: 14 December 2018 Accepted: 31 December 2018 Published: 15 January 2019

---

## Abstract

This paper addressed that graphene is a regular monolayer of carbon atoms settled in a 2D-hexagonal lattice; which is listed among the strongest material ever measured with strength exceeding more than hundred times of steel. However, the strength of graphene is critically influenced by temperature, geometric vacancy defects (VD). Defects are at all believed to worsen the mechanical toughness and reduce the strength of graphene sheet. They are revealed that stiffness and strength are the key factors in determining solidity and life span of any technological devices. Molecular dynamics-based atomistic modeling was performed to predict and quantify the effect of non-bonded interactions on the failure morphology of vacancy affected sheets of graphene. The defective sheet of graphene containing vacancy defect was simulated in conjunction with the non-bonded interactions experienced due to the presence of a pristine sheet of graphene.

---

**Index terms**— graphene, vacancy defects, fracture strength, molecular dynamics simulation, failure morphology.

## 1 Introduction

Graphene is an outstanding material which has a number of multifunctional properties that repeatedly gross it into the title of "wonder material" which is a road map on the way to guide the community toward the development of products [1]. The remarkable mechanical behavior and properties of graphene-based material's has concerned with important study concern in recent years, in line for to their encouraging forecasts, now adaptable divisions for example micromechanics [2], microelectronics [3], and thermal [4] application with desired mechanical properties, and electrical conductivities [2][3][4]. The trial and hypothetical revision of graphene, two-dimensional (2D), is a tremendously growing field of today's condensed matter research. The causes for this massive methodical attention were diverse; on the other hand, one might highlight some key inspirations. Keeping given of the science-based interest generated via graphene and its promising upcoming contribution toward electronic engineering and sensing applications, so a group of research effort is steadfastly hooked on considering the configuration and properties of graphene in this paper. Outstanding toward its excellent mechanical behavior, thermal and electrical conductivities of graphene could also use for more conventional purposes as compared with carbon nanotubes, which was quit restricted to aerospace industries and graphene is also known to have very high stiffness in addition strength until now an extensive scatter have been witnessed in the mechanical properties [1][2][3][4]. In this effort, we present molecular dynamics model simulation for the initiation of defects and the influence of different defects (vacancy defects) and pristine one on mechanical strength of graphene sheets were observed and, the fracture strength was predicted from the numerical simulation and the properties of graphene in table 1 and investigated young's modulus displayed in table 2 below.

Table ??: Properties for a Single Sheet of Graphene [1].

## 2 Property Value

Young's modulus [1] 1.0TPa

44 Rupture strength [1] 130GPa  
 45 Tensile strength [2] 100GPa Thermal conductivity [3][4] 5000w/mK Shear modulus [5][6] 280GPa Longitudinal  
 46 sound velocity [5,[7][8][9] 20km/s Melting temperature [5,10] 4900K Specific surface area [11] 2630m<sup>2</sup> /g Optical  
 47 transmittance [12] 97.70% High electron mobility [13] 250,000cm

### 48 3 Modeling and Methodology a) Molecular Dynamics based 49 Simulation

50 Molecular dynamics-based simulations were performed to study the effect of non-bonded interactions on the  
 51 mechanical behavior and failure morphology of defective graphene sheet. The success of any molecular dynamics-  
 52 based simulations entirely depends on the interatomic potentials chosen for simulating the atomic interactions.  
 53 A Significant amount of advancement in conjunction with computational techniques has already been made  
 54 by the researchers in developing potentials for capturing the realistic properties for the range of materials. In  
 55 this study, AIBO (adaptive intermolecular reactive bond order) potential was used to compute the interatomic  
 56 forces between carbon atoms in graphene. Simulations were performed with a single cutoff distance of 1.95Å as  
 57 proposed in the work of [25]. AIREBO potential consists of a summation of pair potential REBO (E<sub>ij</sub> REBO  
 58 ), non-bonded Lennard Jones potential (E<sub>ij</sub> LJ ) and torsional component between carbon atoms (E<sub>ijk</sub> tors ),  
 59 also described with the help of mathematical expressions in equation (1)., , ,1 2AIREBO REBO LJ ltors ij ij kij  
 60  $E = E_{REBO} + E_{LJ} + E_{tors} + E_{AIBO}$  (1)

61 Here, i, j, k, and l refers to individual atoms, E is the total potential energy of the system estimated with the  
 62 help of AIBO potential. To perform this study, a graphene sheet consisting of 800 atoms was generated in the  
 63 simulation box. The dimensions of a single sheet of graphene was kept fixed at A=46.599Å and B=49.19Å (as  
 64 shown in Fig. 1) along the zig-zag and arm chair direction respectively. In-plane periodic boundary conditions  
 65 were imposed on the simulation box. The interlayer spacing between the sheets of graphene in bilayer graphene  
 66 was kept constant at 3.45Å. During the simulations, the NPT (isothermalisobaric) ensemble in conjunction with  
 67 an integration time step of 1fs was enforced. After achieving a minimum energy configuration of graphene, atoms  
 68 at a temperature of 1K, tensile loading was applied at a strain rate of 0.005ps<sup>-1</sup>. To avoid thermal effects on  
 69 the failure mechanism of graphene, simulations were performed at such a low temperature of 1K. Stress-strain response was estimated in this  
 70 study with the help of the virial stress component [26,27], which can be calculated with the help of mathematical  
 71 expression given in equation (2).  
 72  $\sigma_{ij} = \frac{1}{V} \sum_k m_k v_{ki} v_{kj} - \frac{1}{V} \sum_{k,l} \frac{r_{kl}^i r_{kl}^j}{r_{kl}^3} \phi(r_{kl})$  (2)

73 Here, i and j denote indices in Cartesian coordinates system; ?? and ?? are the atomic indices; ?? ?? and ??  
 74 ?? are mass and velocity of atom ?;?? is the distance between ?? atoms and V is the surrounding  
 75 volume of atom ?. Figure ??: Snapshots on the way to confirm the mathematical method, the fracture strength  
 76 of a pristine graphene sheet was initially calculated. Stress-strain bends of pristine graphene sheet under same  
 77 tension along the zigzag way (black color) and armchair way (red color) at 300K. Now the direction of validating  
 78 the mathematical method, the rupture stress of pure graphene sheet was initially designed. The Consequence of  
 79 minimal stress-strain bend next to the temperature of 300 K, subjected to tension load alongside both armchair  
 80 and zigzag directions shown above Fig. 1, was revealed, that fracture stress beside the armchair and the zigzag  
 81 way are calculated as 91 and 106 GPa, separately. In Cauchy stress; the rupture stiffness was 100GPa and 126  
 82 GPa, and the rupture strain is 0.13 and 0.22 correspondingly. These results were promising new examination,  
 83 i.e., 130 GPa and 130:25 [28] as well as previous numerical simulation [29], verifying dynamism and  
 84 exactness of our mathematical approach.

85 Also, graphene can be subjected to a higher temperature at the production stage as well as when graphene-  
 86 based devices operate at the higher temperature. As we discussed above Chemical vapor deposition (CVD) is  
 87 one of the most commonly used methods of graphene manufacture; that products graphene at a temperature of  
 88 around 800 K. Therefore, understanding the temperature behavior of graphene helps to fabricate best excellence  
 89 graphene founded devices. Studying the effect of high temperature on mechanical properties of a substantial  
 90 armchair and zigzag is presented. In the temperature range of 200K, 300K, and 450K, the breakage stress with  
 91 a vacancy III.

## 92 4 Results and Discussion

93 Molecular dynamics-based simulations were performed to capture the failure morphology of pristine graphene  
 94 either as a single or in bi-layer sheet configuration. These simulations were performed with the help of three  
 95 models to study the effects of nonbonded interactions on the mechanical behavior of pristine graphene. Stress  
 96 and strain response estimated along the zig-zag and arm chair directions of pristine single sheet graphene were  
 97 plotted in Fig. 4. It can be observed from Fig. 4 that the mechanical properties of pristine graphene along with  
 98 the zig-zag and arm chair directions are quite different because of edge defects. In direction to get a better insight  
 99 on the failure mechanism of the pristine form of graphene under the influence of tensile loading, snapshots of the  
 100 simulation box were taken at the time of initiation of the failure as provided in Fig. 4. It is observed that the  
 101 failure morphology of graphene sheet inferred from the snapshots provided in Fig. 4 is almost independent of the  
 102 non-bonded interactions. A brittle nature of failure can be observed in zig-zag as well as arm chair directions of  
 103 graphene sheets under the influence of tensile loading.

---

104 Stress and strain response estimated along with the zig-zag and arm chair directions of pristine single sheet  
105 graphene & bi-layer with (LJ-On) & (LJ-Off) were plotted in Fig. 5 below. It can be observed from Fig. 5 that  
106 the mechanical properties of pristine graphene single & bi-layer along the zig zag and arm chair direction. where  
107 SG (single graphene sheet), BG (LJ-On) (bilayer graphene sheet with non-bonded interactions) and BG (LJ-Off)  
108 (bilayer graphene without non-bonded interactions) [24].

109 It can be inferred from Fig. 6 that non-bonded interactions as well as stiffness of pristine graphene have an  
110 impact on the failure morphology of defective graphene sheet containing single vacancy defects. Snapshots of the  
111 simulation box provided in Fig. 6 (c3) for defective graphene sheet accompanied by a pristine sheet of graphene  
112 connected with non-bonded interactions show that the failure initiates at two different regions subsequently and  
113 helps in achieving higher failure strength. This initiation of failure at two different defects helps in distributing  
114 the energy among these points, which can be attributed to the higher failure strength for defective graphene  
115 sheets in bilayer configuration connected with non-bonded interactions. In the way to investigate the reasons  
116 behind the improvement in the fracture strength and strain of defective graphene in bilayer configuration of  
117 graphene, snapshots at the time of initiation of failure are provided in Fig. 7. It can be observed in Fig. 6  
118 (b3 and c3) that at the higher concentration of single vacancy defects failure triggers from the vacancies at two  
119 separate locations. Distribution of loading with the help of nonbonded interactions as well as pristine graphene  
120 sheet accompanied the defective graphene can be attributed to the higher strength of defective graphene in bi-  
121 layer sheets of graphene. This subsection of the molecular dynamics based simulation helps in concluding that  
122 at higher percentage of single vacancy defects, bilayer sheets of graphene shows higher strength and strain values  
123 for the failure of defective graphene sheet. Improvement in the strength of defective sheet was observed in the  
124 presence of another pristine graphene connected with non-bonded interactions, but no transition from brittle  
125 behavior was observed in any of the failure morphology.

## 126 5 a) Result of single, double and multiple vacancy defects

127 Failure morphology of the single graphene with uniformly distributed vacancies during strain failure vs vacancy  
128 defect ratio was displayed in Fig. 7. A very instance concentrated stress occurred near unperfected; at that  
129 moment breakages happen to open from where vacancy defect started then growth in the (a3) (b3) (c3)  
130 defects.

131 direction of nearby defects where fracture starts randomly from the defect of vacancies exist. We now turn  
132 to analyze the mechanical properties at the failure point for defective graphene. It should be noted that the  
133 ultimate strength is the maximum stress in the stress-strain curves, while the fracture strain is determined from  
134 the spontaneous large drop of the total energy increment curves. Without defect, the ultimate tensile strength  
135 is 91 GPa and 106 GPa intended for armchair and zigzag graphene separately. On behalf of through evenly  
136 concentrated defects, the correlation among stress, strains besides defects are revealed below & (b). Obviously,  
137 the stress decreases with the increase in vacancy defect, and the strain failure decreases with increase vacancy  
138 defect. On or after this we decided that in contrast, stiffness to some extent drops by the rising in vacancy Fig.  
139 8 (b) defect; because lack of an atom implies vacancy defect that graphene is more sensitive to vacancy where  
140 carbon bond breakage is happens at the time.

141 This study revealed that fracture stress in zig zag direction with different single, double, and multiple vacancy  
142 defects are much better in Pristine single graphene than bilayer di-vacancy, single bilayer vacancy (dangling bond  
143 because of odd vacancy defect) and multi-vacancy defect in bilayer single graphene defects are also shown in this  
144 bar graph below Fig. ??.

## 145 6 Figure 9:

146 Fracture stress in zig zag direction with different single, double and multiple vacancy defects. Here, the pristine,  
147 BG, SG, refers to pristine single graphene sheet, bilayer graphene, and single graphene respectively; Whereas,  
148 SV, DV and MV refer to single, di-and multi-vacancy defects.

149 IV.

## 150 7 Conclusions

151 Molecular dynamics-based simulations were performed to predict the effect of non-bonded interactions on the  
152 mechanical behavior and failure morphology of defective graphene sheet. Simulations were performed with an  
153 isolated defective sheet of graphene or defective sheet of graphene accompanied by a pristine sheet of graphene.  
154 Atomistic modeling with single as well as bilayer configuration of graphene was performed with different defect  
155 concentrations as well as geometries of vacancy defects such as single, double, and multiple vacancy defects.  
156 Di-vacancy defects have predicted higher strength in zig-zag configuration, whereas lower strength in arm chair  
157 configuration while compared with the single vacancy defects. A Shift in the failure morphology of graphene  
158 along the arm chair direction was observed in bi-layer configuration of defective graphene containing di-vacancy  
159 defects. It can be concluded that non-bonded interaction helps in achieving a uniform distribution of load around  
160 the defects which triggers the failure simultaneously from different regions & initiating of failure simultaneously  
161 from two different points help in achieving a higher strength.

162 **8 Pristine BG (DV) BG (SV) BG (MV) SG (SV) SG (MV)**

163 Fracture Stress (GPa)

164 Graphene Configuration

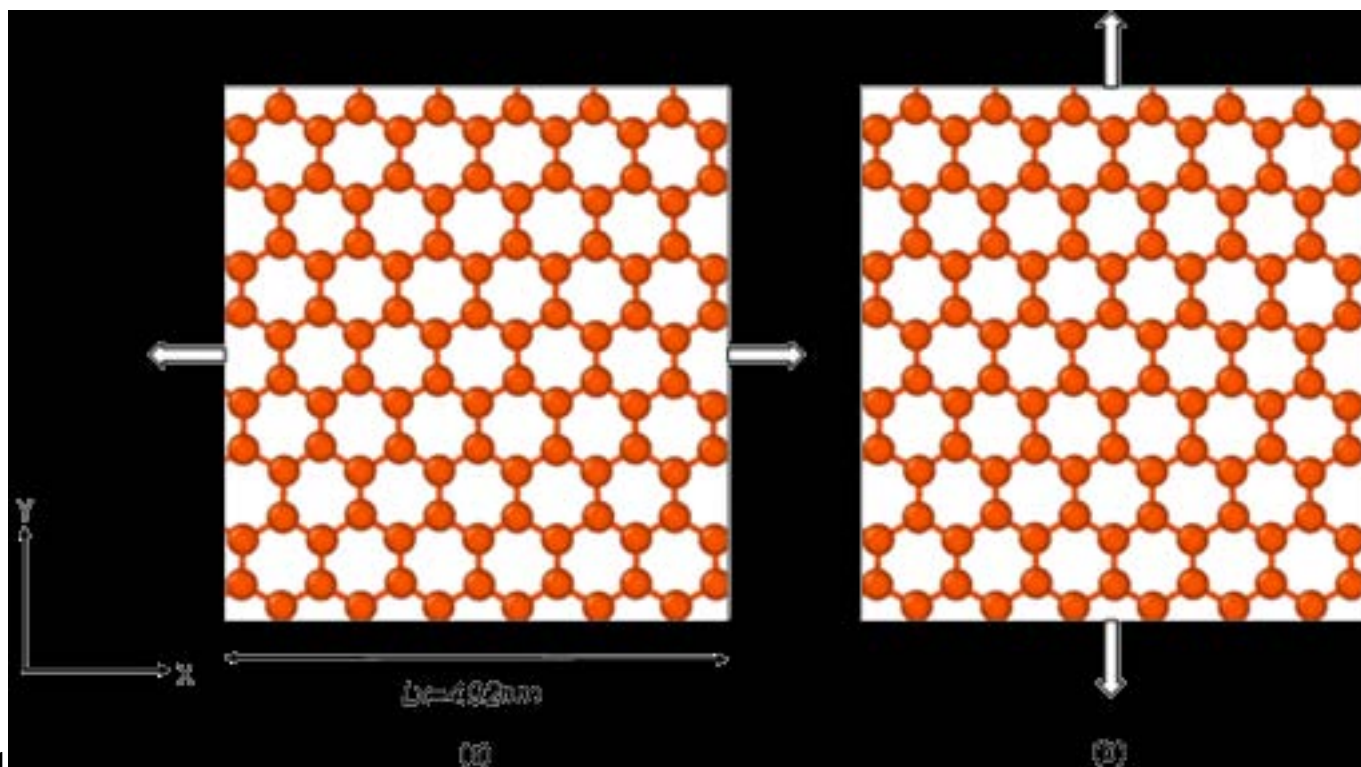


Figure 1: Figure 1 :

165 1

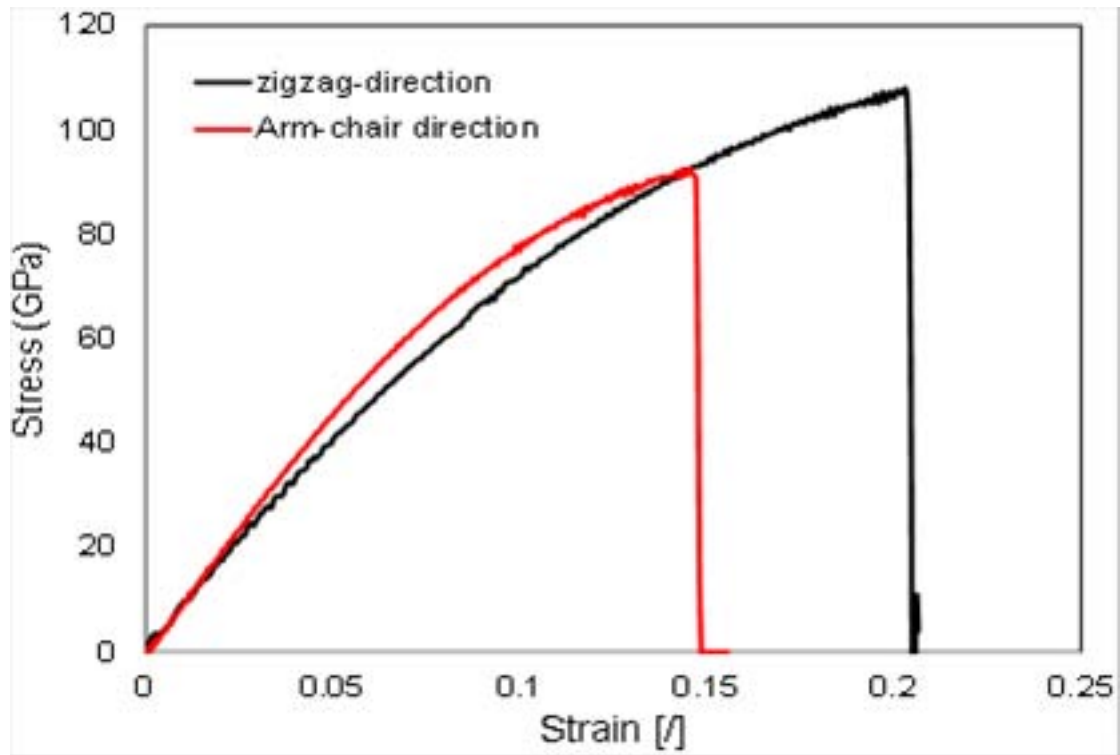
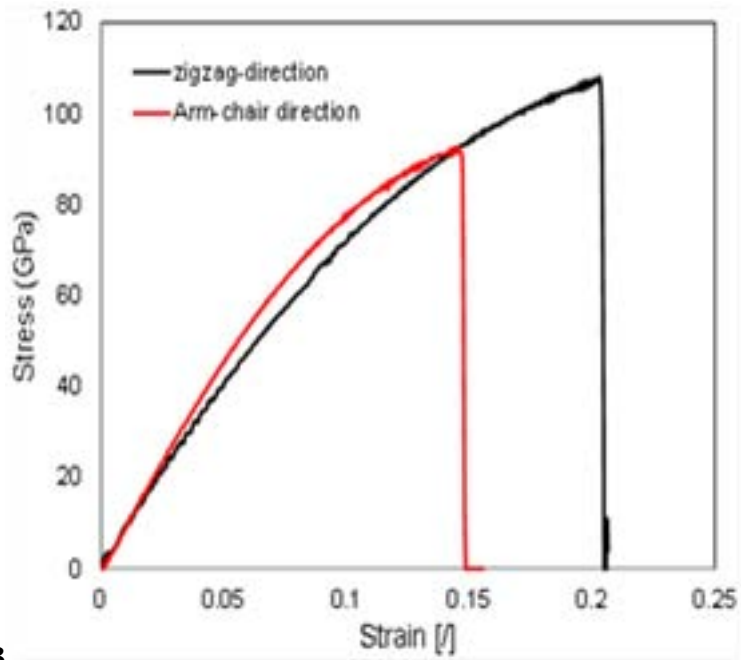


Figure 2: Global



3

Figure 3: Figure 3 :

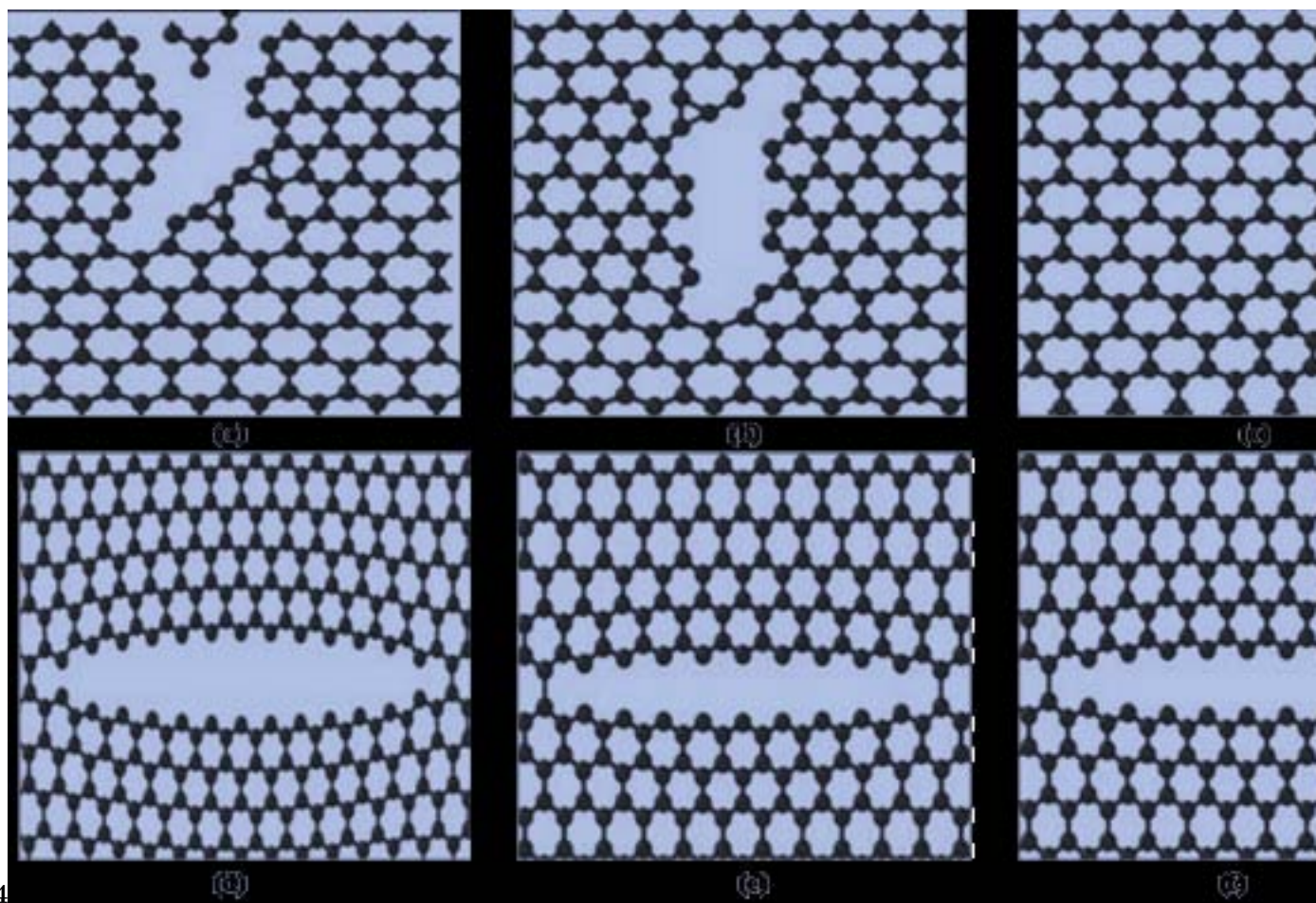


Figure 4: Figure 4 :

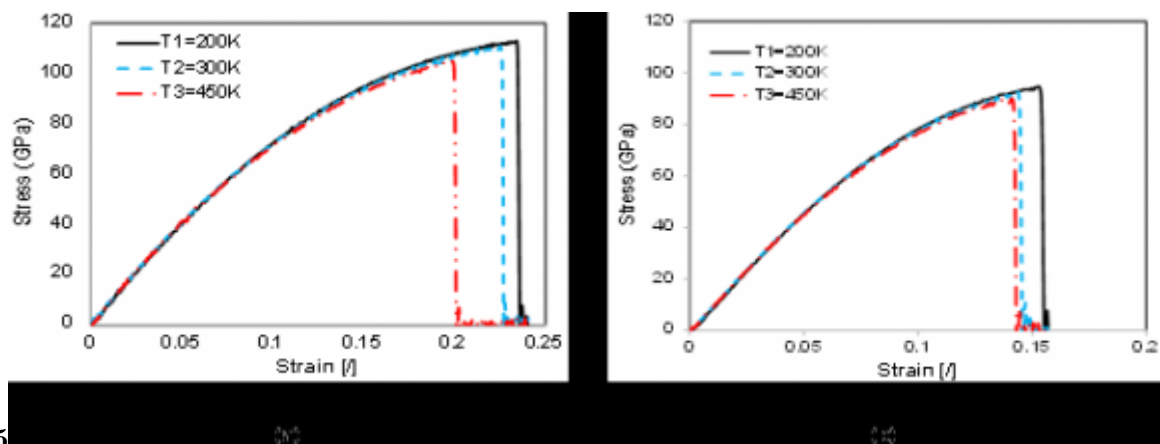


Figure 5: Figure 5 :

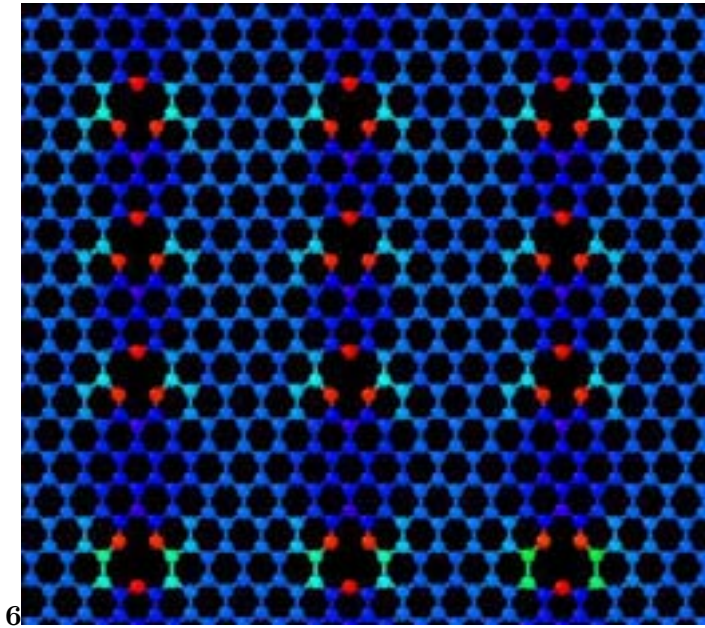


Figure 6: Figure 6 :

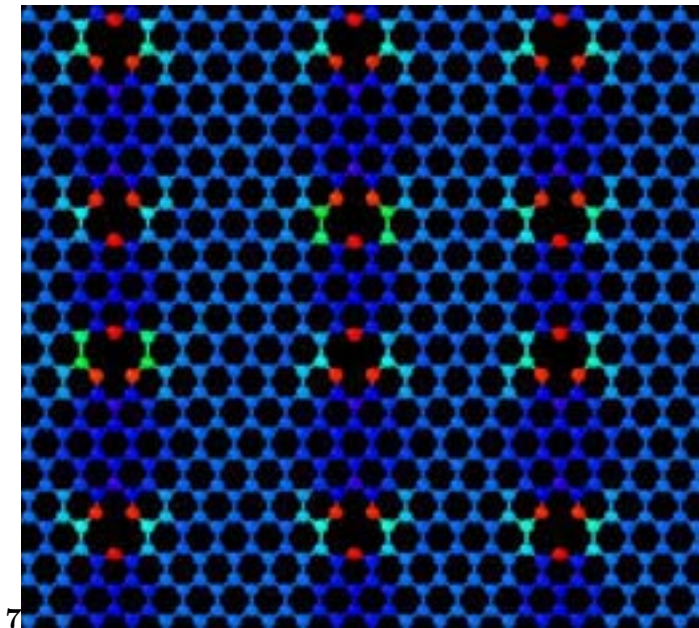


Figure 7: Figure 7 :

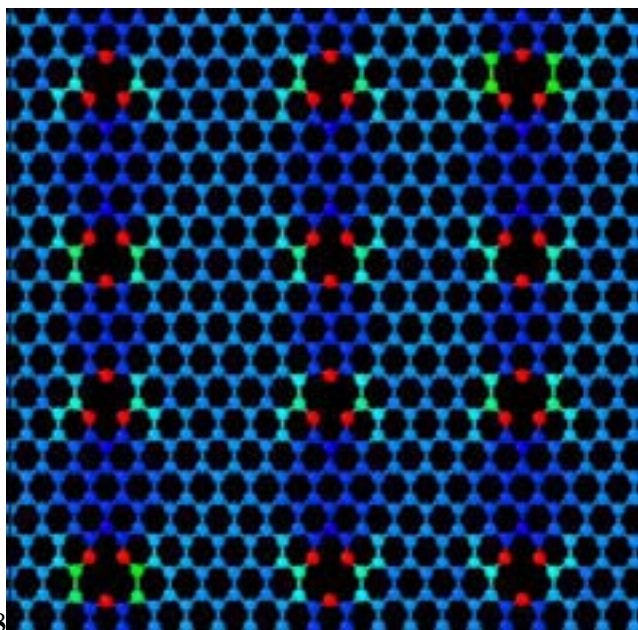


Figure 8: Figure 8 :

Figure 9:

2

Studied by	Conditions/ Defects	Types of	Methods Adopted	Young's Modulus (TPa)	Poisson's Ra- tio
Jiang et al. 14	T = 100-500 K		Molecular Dynamics	0.95 -1.1	0.17
Shen et al . 15	T = 300-700 K		Molecular Dynamics	0.905	
Lee et al. 16	Pristine graphene		Experiment	1 ± 0.1	
Tsai et al .17	NPT ensemble		Molecular Dynamics	0.912	0.261
Sakhaee-Pour 18	Pristine graphene		Finite Element Method	1.025	
Georgantzinos et al. 19	Pristine graphene		Finite Element Method	1.367	
Kvashnin et al. 20	Vacancy defects		Molecular Mechanics	1.08	
Neek-Amal et al. 21	randomly distributed vacancy defects		STW defects	0.501 ± 0.032	
Shokrieh et al. 22	Pristine graphene		Continuum Mechan- ics	1.04	
R.Ansary et al. 23	STW defects		Molecular Dynamics	60% reduction	
Muse Degefe & Avinash Parashar et al. 24 II.	Vacancy bi-layer T=300K graphene		Molecular Dynamics	0.91	

Figure 10: Table 2 :

- 
- 166 [Dmitriev et al. ()] , S V Dmitriev , J A Baimoya , A V Savin , Y S Kivshar . *Comput. Mater. Sci* 2012. 53 p.  
167 .
- 168 [Ni et al. ()] ‘Anisotropic mechanical properties of graphene sheets from molecular dynamics’. Z Ni , H Bu , M  
169 Zou , H Yi , K Bi , Y Chen . *Physica B* 2010. 405 p. .
- 170 [Tsai and Tu ()] ‘Characterizing mechanical properties of graphite using molecular dynamics simulation’. J L  
171 Tsai , J F Tu . *Mater. Des* 2010. 31 p. .
- 172 [Cummings et al.] ‘Charge Transport in Polycrystalline Graphene: Challenges and Opportunities’. A W Cum-  
173 mings , D L Duong , V L Nguyen , D V Tuan , J Kotakoski , J E B Varga . *Adv. Mater* 26 p. .
- 174 [Degefe and Parashar ()] ‘Effect of nonbonded interactions on failure morphology of a defective graphene sheet’.  
175 M Degefe , A Parashar . *Materials Research Express* 2016. 3 (4) p. 45009.
- 176 [Rajasekeran et al. ()] ‘Effect of Point and Line Defects on Mechanical and Thermal Properties of Graphene:  
177 A Review’. G Rajasekeran , Avinash Prarthana Narayanan , Parashar . *Critical Reviews in Solid State and*  
178 *Materials Sciences* 2015. p. .
- 179 [Sakhaee-Pour ()] ‘Elastic properties of single-layered graphene sheet’. Sakhaee-Pour . *Solid State Commun* 2009.  
180 149 p. .
- 181 [Lv et al. ()] ‘Graphene-DNA hybrids: self-assembly and electrochemical detection performance’. Wei Lv , Min  
182 Guo , Ming-Hui Liang , Feng-Min Jin , Lan Cui , Linjie Zhi , Quan-Hong Yang . *J. Mater. Chem* 2010. 20  
183 (32) p. .
- 184 [Tu et al. ()] ‘Lee structures of thermally and chemically reduced graphenes’. H M Tu , S H Huh , S H Choi ,  
185 HL . *Mater-lett* 2010. 64.
- 186 [Tu et al. ()] ‘Lee structures of thermally and chemically reduced graphenes’. H M Tu , S H Huh , S H Choi ,  
187 HL . *Mater-lett* 2010. 64.
- 188 [Peters ()] ‘Linear reduction of stiff-ness and vibration frequencies in defected circular monolayer graphene’. M ,  
189 F M Peters . *Phys. Rev. B Condens. Matter* 2010. 81 p. 235437.
- 190 [Lee et al. ()] ‘Measurement of the elastic properties and intrinsic strength of monolayer graphene’. C Lee , X  
191 Wei , J W Kysar , J Hone . *Science* 2008. 321 p. .
- 192 [Lee et al. ()] ‘Measurement of the elastic properties and intrinsic strength of monolayer graphene’. C Lee , X  
193 Wei , J W Kysar , J Hone . *Science* 2008. 321 p. .
- 194 [Ansari et al. ()] *Mechanical properties of defective single-layered graphene sheets via molecular dynamics*  
195 *simulation, Super lattices Microstructure*, R Ansari , S Ajori , B Motevalli . 2012. 51 p. .
- 196 [Frank et al. ()] ‘Mechanical properties of suspended graphene sheets’. W Frank , D M Tanenbaum , A M Van  
197 Der Zande , P L Mc Euen . *J. Vac. Sci. Technol. B* 2007. 25 p. .
- 198 [Liu et al. ()] ‘Morphology and in-plane thermal conductivity of hybrid graphene sheets’. Bo Liu , C D Reddy ,  
199 Jinwu Jiang , Julia A Baimova , V Sergey , Ayrat A Dmitriev , Kun Nazarov , Zhou . *Applied Physics Letters*  
200 2012. 101 (21) p. 211909.
- 201 [Parashar and Mertiny ()] ‘Multiscale model to investigate the effect of graphene on the fracture characteristics  
202 of graphene/polymer nanocomposites’. Avinash Parashar , Pierre Mertiny . *Nanoscale research letters* 2012.  
203 7 (1) p. .
- 204 [Parashar and Mertiny ()] ‘Multiscale model to investigate the effect of graphene on the fracture characteristics  
205 of graphene/polymer nanocomposites’. Avinash Parashar , Pierre Mertiny . *Nanoscale research letters* 2012.  
206 7 (1) p. .
- 207 [An et al. ()] ‘Observation of electron-antineutrino disappearance at Daya Bay’. F P An , J Z Bai , A B Balantekin  
208 , H R Band , D Beavis , W Beriguete , M Bishai . *Physical Review Letters* 2012. 108 (17) p. 171803.
- 209 [Mohr et al. ()] ‘Phonon dispersion of graphite by inelastic x-ray scattering’. M Mohr , J Maultzsch , E Dobard?  
210 ? , S Reich , I Milo?evi? , M Damnjanovi? , A Bosak , M Krisch , C Thomsen . *Physical Review B* 2007. 76  
211 (3) p. 35439.
- 212 [Shokrieh and Rafiee ()] ‘Prediction of Young’s modulus of graphene sheets and carbon nanotubes using  
213 nanoscale continuum mechanics approach’. M Shokrieh , R Rafiee . *Mater. Des* 2010. 31 p. .
- 214 [Parashar and Mertiny ()] ‘Representative volume element to estimate buckling behavior of graphene/polymer  
215 nanocomposites’. P Parashar , Mertiny . *Nanoscale Res. Lett* 2012. 7 p. 515.
- 216 [Fennimore et al. ()] ‘Rotational actuators based on carbon nanotubes’. A M Fennimore , T D Yuzvinsky , Wei-  
217 Qiang Han , M S Fuhrer , J Cumings , A Zettl . *Nature* 2003. 424 (6947) p. .
- 218 [Los et al. ()] ‘Scaling properties of flexible membranes from atomistic simulations: application to graphene’. J  
219 H Los , I Mikhail , O V Katsnelson , K V Yazyev , Annalisa Zakharchenko , Fasolino . *Physical Review B*  
220 2009. 80 (12) p. 121405.

- 221 [Shen et al. ()] ‘Temperaturedependent elastic properties of single layer graphene sheets’. L Shen , H S Shen , C  
222 L Zhang . *Mater. Des* 2010. 31 p. .
- 223 [Novoselov et al. ()] ‘Two-dimensional atomic crystals’. K S Novoselov , D Jiang , F Schedin , T J Booth , V  
224 V Khotkevich , S V Morozov , A K Geim . *Proceedings of the National Academy of Sciences of the United*  
225 *States of America* 2005. 102 (30) p. .
- 226 [Novoselov et al. ()] ‘Two-dimensional atomic crystals’. K S Novoselov , D Jiang , F Schedin , T J Booth , V  
227 V Khotkevich , S V Morozov , A K Geim . *Proceedings of the National Academy of Sciences of the United*  
228 *States of America* 2005. 102 (30) p. .
- 229 [Gillen et al. ()] ‘Vibrational properties of graphene nanoribbons by first-principles calculations’. Roland Gillen  
230 , Marcel Mohr , Christian Thomsen , Janinamaultzsch . *Physical Review B* 2009. 80 (15) p. 155418.
- 231 [Jiang et al. ()] ‘Young’s modulus of Graphene: a molecular dynamics study’. W Jiang , J S Wang , B Li . *Phys.*  
232 *Rev. B Condens. Matter* 2009. 80 p. 113405.